Three-State Denaturation of DnaK Induced by Guanidine Hydrochloride. Evidence for an Expandable Intermediate†

Daniel R. Palleros, Li Shi, Katherine L. Reid, and Anthony L. Fink*

Department of Chemistry and Biochemistry, University of California, Santa Cruz, California 95064

Received December 9, 1992; Revised Manuscript Received February 16, 1993

ABSTRACT: The denaturation of the heat shock protein DnaK induced by guanidine hydrochloride (Gdn·HCl) was investigated by circular dichroism, fluorescence, size-exclusion HPLC, and dynamic light scattering. DnaK unfolding takes place in two discrete steps. The midpoint (C_m) of the first transition (0.5 M) was shifted to higher denaturant concentrations (0.8 M) in the presence of Mg/ADP or Mg/ATP, whereas the second transition (C_m = 1.6 M) was unaffected by nucleotides. An intermediate state which continuously expands with increasing Gdn·HCl concentration was observed; its relation to molten globules is discussed. In addition, a direct correlation between molecular volume and ellipticity at 222 nm was found, regardless of the conformational state (native, intermediate, unfolded); the implications of these findings are discussed. The unfolding of DnaK is best explained by a hierarchical model of unfolding.

DnaK, the only *Escherichia coli* member of the 70-kDa family of heat shock proteins (hsp70), has been shown to interact with unfolded polypeptide chains (Liberek et al., 1991; Sherman & Goldberg, 1991; Landry et al., 1992; Palleros et al., 1992) and is able to reactivate aggregated proteins (Skowyra et al., 1990). It has also been shown that DnaK in the presence of DnaJ and GrpE proteins, assists the renaturation of λcI857 mutant protein (Gaitanaris et al., 1990). It has been recently demonstrated in in vitro experiments that DnaK, in conjunction with DnaJ, GrpE and GroEL in a successive manner, catalyzes the refolding of rhodanese (Langer et al.,1992).

In order to study the interactions of unfolded proteins with molecular chaperones such as DnaK, hsp73, or GroEL, it is necessary to denature the substrate polypeptide chain under conditions in which the molecular chaperone remains active. This has been accomplished by permanent disruption of the the polypeptide structure by modification of disulfide bonds (Palleros et al., 1991, 1992; Langer et al., 1992) or by inducing thermal denaturation of unstable proteins (Palleros et al., 1991). However, when a more general approach, such as the addition of denaturants, is used, an understanding of the stability of the molecular chaperones under such conditions is necessary. In this paper we studied the stability of DnaK in the presence of Gdn·HCl[1] by far-UV CD, fluorescence spectroscopy, size-exclusion HPLC, dynamic light scattering, and binding of the fluorescence probe bis-ANS.

Members of the hsp70 family posses two functional domains (Chappell et al., 1987; Flaherty et al., 1990): a 44-kDa N-terminal domain, which is responsible for ATP and ADP binding and which has been highly conserved throughout evolution, and a more variable C-terminal domain. The N-terminal domain consists of two lobes, each of which can in turn be subdivided into two subdomains. The nucleotides bind at the base of the cleft separating the lobes (Flaherty et al., 1990, 1991). It was found that the overall structure of the N-terminal domain is similar to that of actin and yeast hexokinase even though these proteins have a low degree of sequence identity (Flaherty et al., 1990). We previously investigated the effect of temperature on the stability of DnaK and bovine brain hsp73 (hsc70) (Palleros et al., 1991, 1992). We found that both proteins undergo a biphasic transition as the temperature is increased. In the absence of nucleotides, DnaK and hsp73 partially unfold to an intermediate state (midpoint of the transition: 41–42 °C) which has the characteristics of a molten globule state [i.e., a compact denatured state with a high degree of secondary structure and fluctuating tertiary structure; for reviews, see Ptitsyn (1992), Kuwajima (1989), Christensen and Pain (1991), and Baldwin (1991)]. The intermediate state of hsp73 irreversibly aggregates, while the compact denatured state of DnaK refolds to its native conformation upon cooling. For both proteins a second transition takes place at higher temperatures (midpoint: 71 °C (DnaK), 65 °C (hsp73)) that leads to a species with some residual secondary structure even at 90 °C (Palleros et al., 1992).

The existence of compact denatured states (molten globules) has been clearly shown at low pH. However, under equilibrium conditions in the presence of Gdn·HCl or urea, their existence has mainly been inferred by the lack of coincidence of the transition midpoints, or C_m values, by different spectral probes (Robson & Pain, 1976; Creighton & Pain, 1980; Mitchinson & Pain, 1985; Ptitsyn et al., 1990; Matthews & Crisanti, 1981; Yutani & Ogasahara, 1980; Kuwajima et al., 1976; Nozaka et al., 1978; Zerovnik et al., 1992; Nozais et al., 1992; Mitraki et al., 1987; Lehrman et al., 1991; Saito & Wada, 1983); only in a few instances was the intermediate the only species present in a given range of denaturant concentration (Saito & Wada, 1983; Robson & Pain, 1976). This fact, together with the occurrence of aggregation processes observed for some proteins (Ptitsyn et al., 1990; Cleland & Wang, 1990; Nozais et al., 1992), precluded a full characterization of the equilibrium intermediate state formed in the presence of denaturants such as urea or Gdn·HCl. Studies on the hydrodynamic properties of these states are scarce (Ptitsyn et al., 1990). In this paper, we present clear evidence of the existence of a stable equilibrium intermediate for DnaK which can be isolated in the range 0.6–1.0 M Gdn·HCl.

† This work was supported by NIH Grant RO1 GM45316.

* To whom correspondence should be addressed.

[1] Abbreviations: Gdn·HCl, guanidine hydrochloride; Bis-ANS, 1,1′-bis(4-anilino-5-naphthalenesulfonic acid); hsp, heat shock protein; EDTA, ethylenediaminetetraacetic acid; SDS, sodium dodecyl sulfate; DTT, dithiothreitol; PAGE, polyacrylamide gel electrophoresis; SEC, size-exclusion chromatography; HPLC, high-performance liquid chromatography; CD, circular dichroism; DLS, dynamic light scattering.

0006-2960/93/0432-4314$04.00/0

EXPERIMENTAL PROCEDURES

Materials. *E. coli* DnaK was isolated and purified by a modification of procedures previously described (McCarty & Walker, 1991; Cegielska & Georgopoulos, 1989). Our protocol omits the heparin–agarose purification step and the final gel-permeation step, since it was found that these steps did not contribute significantly to the purification; instead we added a final ammonium sulfate precipitation step. The final purity of DnaK was greater than 98% as determined by SDS–PAGE (Coomassie blue staining), deemed adequate for the present study. DnaK stock solutions were 13–27 μM in buffer Q (25 mM Hepes, pH 7.6 with KOH, 50 mM KCl, 1 mM EDTA, 5mM 2-mercaptoethanol, and 10% (v/v) glycerol). The DnaK molar extinction coefficient at 280 nm (27 000 $M^{-1}cm^{-1}$) was determined by measuring the absorbance of DnaK solutions whose concentrations in mg/mL were assayed with a Pierce BCA protein assay reagent kit using bovine serum albumin as standard. 1,1′-Bis(4-anilino-5-naphthalenesulfonic acid), dipotassium salt (bis-ANS), was from Molecular Probes Inc. (Eugene, OR). Gdn·HCl, ultrapure grade, was from ICN Biochemicals. ATP (disodium salt) was from Pharmacia LKB Biotechnology Inc.; ADP (monosodium salt) was from Calbiochem. All other chemicals were from the same sources as already reported (Palleros et al., 1992).

Methods. Far-UV circular dichroism and fluorescence spectroscopy were performed as already described (Palleros et al., 1992). DnaK mean residue weight ellipticities reported here are larger than those previously published (Palleros et al., 1992); the discrepancy arises from a previous overestimation of DnaK concentration. SDS–PAGE experiments were performed using a Pharmacia Phast system. Guanidine hydrochloride concentrations were determined by index of refraction as described elsewhere (Nozaki, 1972), using a Bausch & Lomb refractometer. UV-visible absorbance measurements were performed on a Hewlett-Packard 8452A diode array spectrophotometer.

Unfolding Transitions. Unfolding curves were determined by successive addition of small aliquots of 8 M Gdn·HCl solution in buffer P (100 mM sodium phosphate and 0.20 M KCl, pH 6.5) to a 1 μM DnaK solution in the same buffer with 1 mM dithiothreitol. After each addition, the ellipticity at 222 nm or the fluorescence intensity at 335 nm (excitation: 280 nm) was monitored as a function of time until it reached a constant value (less than 20 min in all cases). Then the spectrum at each Gdn·HCl concentration was determined. Values reported in Figures 1B and 2B are corrected by the dilution caused by the addition of the denaturant. Each experiment was run at least twice; averaged values are reported. Identical results were obtained when samples at different denaturant concentrations were prepared individually.

Size-Exclusion HPLC. HPLC experiments were carried out at 23 ± 1 °C as previously reported (Palleros et al., 1992), using a Bio-Sil SEC-250 silica column (600 × 7.8 mm; Bio-Rad, Richmond, CA) and a two-pump HPLC system, equilibrated with buffer P and 6 M Gdn·HCl in buffer P. Buffers from each pump were delivered at different rates to generate the denaturant concentrations indicated in Figures 3 and 4; flow rate was 1 mL/min. Gdn·HCl concentration was determined by measuring the index of refraction of the eluent. Detection was by absorbance at 215 nm. DnaK solutions (4 μM), containing blue dextran and sodium azide, at different denaturant concentrations were prepared at room temperature (23 ± 1 °C) 10 min before injection; 20–200-μL aliquots were injected into the HPLC system. Chromatograms were collected on a computer with acquisition time 1 point/sec. For each species, the areas under the curves were obtained by curve fitting of the chromatogram with the program LabCalc (Galactic Industries, Salem, NH), using Gaussian functions. Partition coefficients were calculated as $K_d = (V_i - V_o)/V_t$, where V_i is the protein elution volume, V_o is the void volume (elution volume of blue dextran), and V_t is the total solvent-accessible volume (elution volume of sodium azide).

Bis-ANS Binding. Experiments were performed as follows: DnaK stock solution (26.7 μM, in buffer Q) aliquots (26 μL) were mixed with 20 μL of bis-ANS stock solution (48 μM in 100 mM Tris-HCl, pH 7.5; concentration was determined by absorbance at 395 nm, ϵ = 16 000 M^{-1} cm^{-1}), 5.1 μL of DTT stock solution (136 mM in 100 mM Tris-HCl, pH 7.5), and varying volumes (0–147 μL) of 8 M Gdn·HCl solution in buffer P, and the volume was made up to 700 μL by adding buffer P. The mixtures were equilibrated at 20.0 °C for 2 h before the fluorescence spectra were scanned (410–600 nm) with excitation at 394 nm.

Dynamic Light Scattering (DLS). Measurements were made at 25.0 ± 0.1 °C using an argon ion laser (488 nm) from Spectra-Physics (Mountain View, CA) and a 128-channel photon correlator spectrometer (Brookhaven Instruments Corporation, Ronkonkoma, NY). The intensity autocorrelation function of the scattered light was measured at three angles (30°, 60°, and 90°). The relaxation spectra were analyzed with the program CONTIN (version 2, 1984) by S. W. Provencher. Sample time was in the range 1.7–20 μs, and acquisition time was 1–50 min (depending on the angle). No dependence of the diffusion coefficient on the scattering angle was observed. Samples were filtered using a Millipore Millex-GV4 (0.22 μm) filter. Protein concentration was 4.5 μM. Viscosity was measured using a Cannon-Ubblohde semi-micro viscometer (Cannon Instrument Co., State College, Pennsylvania) at 25.0 ± 0.1 °C.

RESULTS

Far-UV Circular Dichroism. Figure 1A shows the far-UV CD spectra of DnaK under native conditions and in the presence of Gdn·HCl. The unfolding of DnaK by increasing amounts of the denaturant was followed by the change in ellipticity at 222 nm (Figure 1B). There is a slight decrease in ellipticity at low Gdn·HCl concentrations (<0.3 M) followed by a transition (C_m = 0.50 ± 0.05 M) where only about 15% of the signal at 222 nm is lost. The ellipticity remains rather constant between 0.7 and 1.0 M Gdn·HCl; a second and less cooperative transition is observed between 1 and 2.5 M Gdn·HCl (C_m = 1.6 ± 0.1 M). In the presence of an excess of Mg/ADP, the first transition is shifted to C_m = 0.80 ± 0.05 M Gdn·HCl and the second transition remains unchanged (C_m = 1.61 ± 0.04 M). This process is reversible. For a given final denaturant concentration (0.3–2.5 M), the same CD (and fluorescence) spectrum is obtained regardless of the initial Gdn·HCl concentration (0 or 6 M) in which the protein solution is made.

Unfolding Followed by Fluorescence. Figure 2A shows the fluorescence emission spectra of native DnaK and DnaK in the presence of increasing amounts of denaturant. The native protein shows a maximum at 335 nm. DnaK has only one tryptophan and seven tyrosine residues all located in the N-terminal domain (Bardwell & Craig, 1984). The effects of increasing concentration of the denaturant on the relative intensities at 335 and 305 nm are shown in Figure 2B. In the absence of nucleotides, there is a major transition centered at 0.50 ± 0.01 M Gdn·HCl as detected by tryptophan emission

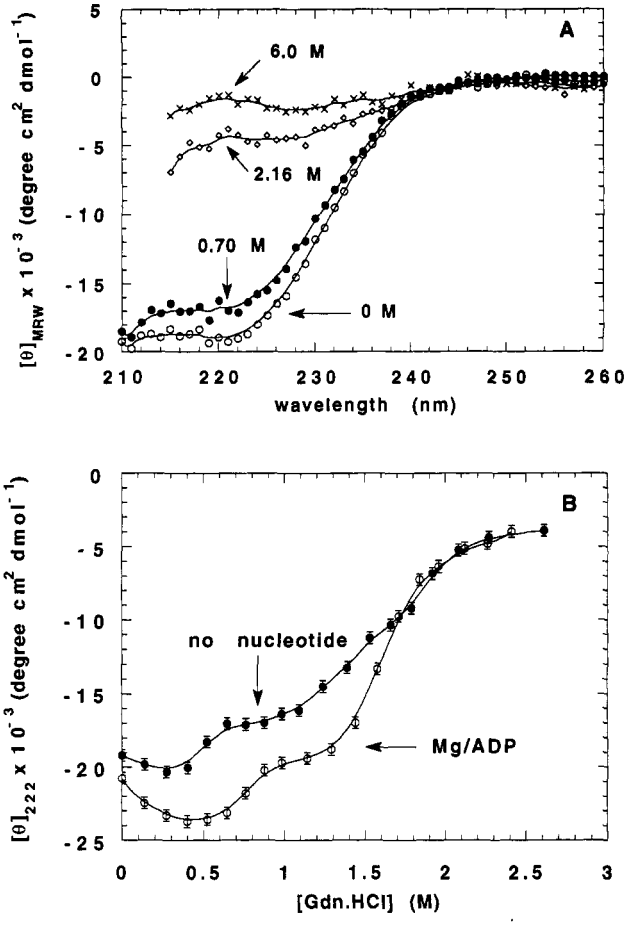

FIGURE 1: Gdn·HCl-induced denaturation of DnaK followed by far-UV CD. (**A**) Far-UV CD spectra at 20.7 °C; protein solutions (1 μM) were in buffer P (100 mM sodium phosphate and 0.20 M KCl, pH 6.5) + 1 mM DTT, at the Gdn·HCl concentrations shown in the figure. (**B**) Unfolding curves at 20.7 °C; closed circles: without nucleotide; open circles: in the presence of Mg/ADP (1 mM).

(335 nm), and there are two transitions (C_m = 0.6 ± 0.1 and 1.5 ± 0.1 M) as indicated by the tyrosine emission (305 nm). The presence of Mg/ADP (or Mg/ATP, not shown) causes a shift in the first transition to C_m = 0.82 ± 0.02 M Gdn·HCl (followed at 335 nm) and no change, within the experimental error, in the C_m (1.8 ± 0.2 M, followed at 305 nm) of the second transition.

Unfolding Followed by Size-Exclusion HPLC. Size-exclusion chromatography (SEC) can be applied to the study of protein folding since it is able to resolve the changes in hydrodynamic properties (Stokes radius) along the denaturation pathway. It is also able to detect the presence of intermediate states provided they are kinetically stable within the time scale of the chromatographic run.

Figure 3 shows the guanidine-induced unfolding of DnaK analyzed by SEC–HPLC at different denaturant concentrations. At [Gdn·HCl] < 0.3 M, DnaK appears as a single peak (N in Figure 3). Between 0.3 and 0.5 M Gdn·HCl a second peak is observed (elution volume: V_e = 13.7–13.5 mL in Figure 3). We call this species I. This new peak becomes more prominent as the Gdn·HCl concentration increases. Between 0.6 and 1.0 M it is the only peak detected. Above 1.1 M the

[2] In this paper we designate the "denatured" state to be any state that involves a major conformational change, as determined by CD or fluorescence, from the native structure and reserve the term "unfolded" state for the ensemble of conformations obtained at high denaturant concentrations.

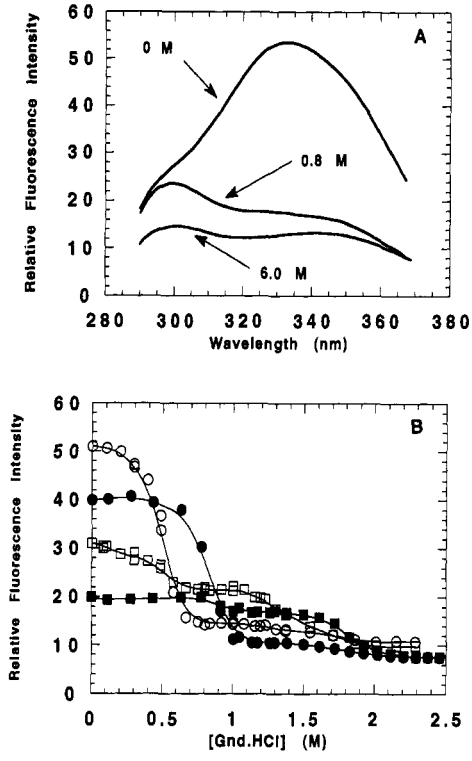

FIGURE 2: Gdn·HCl-induced denaturation of DnaK followed by fluorescence at 20.7 °C; excitation, 280 nm; excitation slit, 4 nm; emission slit, 10 nm. (**A**) Fluorescence spectra in buffer P + 1 mM DDT at the Gdn·HCl concentrations indicated in the figure; [DnaK] = 1 μM. (**B**) Gdn·HCl unfolding curves; circles: followed at 335 nm; squares: followed at 305 nm; open symbols: no nucleotide; closed symbols: in the presence of 0.5 mM Mg/ADP.

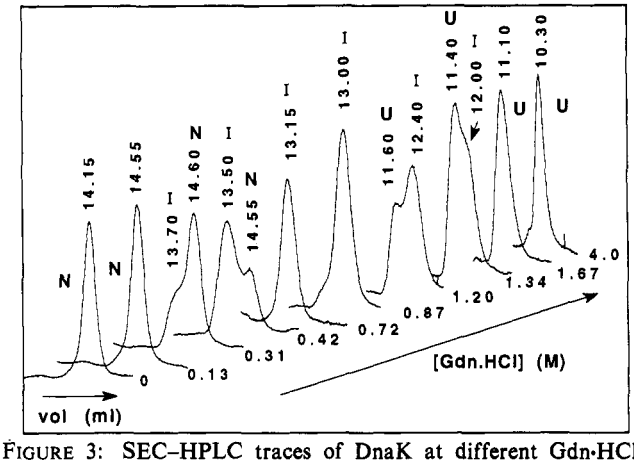

FIGURE 3: SEC–HPLC traces of DnaK at different Gdn·HCl concentrations. Separation was carried out at 23 ± 1 °C. The elution volumes (mL) and the Gdn·HCl concentrations (M) are indicated in the figure.

presence of a new peak is evident; at 1.2 M two species with very close elution volumes (V_e = 11.6 and 12.4 mL in Figure 3) coexist. Above 1.7 M only one peak is detected; we call this species U, the unfolded state.[2] SEC elution volumes are related to the column resolution capabilities through the partition coefficient, K_d. The K_d values for I and U decreased sharply as Gdn·HCl concentration increased, indicating a significant increase in hydrodynamic size with increasing denaturant concentration (see below). The C_m values obtained from SEC peak areas are 0.4 ± 0.1 and 1.4 ± 0.2 M, in agreement, within the experimental error, with those obtained by spectroscopic methods.

The effect of DnaK concentration on the elution volume of I was studied at a fixed concentration of Gdn·HCl in the

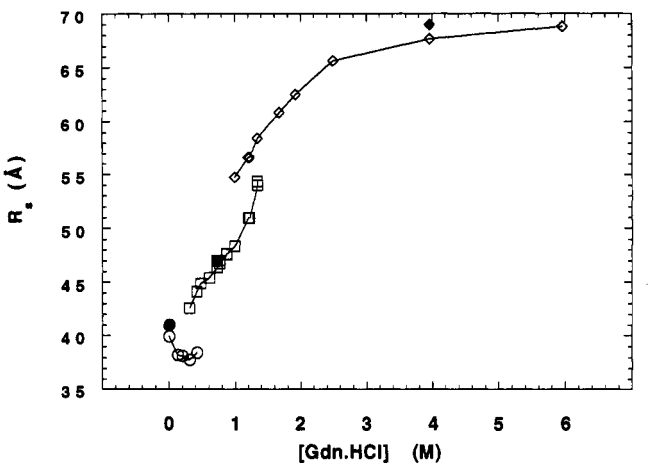

FIGURE 4: Stokes radii of DnaK as a function of Gdn·HCl concentration. DnaK states: circles, native; squares, intermediate; diamonds, unfolded. Open symbols, data from SEC–HPLC determinations; closed symbols, data from DLS experiments (see text).

mobile phase. At Gdn·HCl = 0.6 M, the elution volume of I was essentially unchanged (13.3 ± 0.05 mL) over a range of DnaK concentrations from 1.6 to 72 μM.

The elution volume of DnaK intermediate, I, at Gdn·HCl = 0 M can be determined by inducing the formation of the intermediate with Gdn·HCl and then injecting the sample into the HPLC column equilibrated with buffer without denaturant. The intermediate state characterized under such far-from-equilibrium conditions would be the *kinetic* rather than the *thermodynamic* intermediate. When DnaK was incubated with Gdn·HCl in the concentration range of denaturant of 0.5–1.0 M for 10 min at room temperature and then injected into the HPLC column equilibrated with 20 mM sodium phosphate and 0.20 M KCl, pH 6.5, two peaks coeluted. The peak corresponding to the native protein was at 14.2 ± 0.1 mL, and the peak for the intermediate eluted at 13.5 ± 0.1 mL. This elution volume translates into a Stokes radius (see below) of 43 ± 2 Å.

Stokes Radii. Stokes radii were determined by SEC–HPLC and DLS. K_d values were measured for several standard proteins for which the Stokes radii (R_S) were calculated from intrinsic viscosity measurements [η] (Corbett & Roche, 1984; Tanford, 1968, and references therein) using the relationship $[\eta] = (2.5N/M_r)\times(R_S^3 4\pi/3)$ for rigid spheres, where N is Avogadro's number and M_r is the molecular mass. Standard proteins (Stokes radii in Å) were ribonuclease A (19.3), myoglobin (20.2), bovine serum albumin (33.9), carbonic anhydrase (23.6), and ovalbumin (31.2). A plot of K_d vs log R_S for the standard proteins gave a good linear correlation: $K_d = 1.365 - (0.734 \log R_S)$ ($r = 0.985$). This equation was used to estimate R_S for DnaK as a function of Gdn·HCl. R_S values of DnaK at three different points in the unfolding pathway ([Gdn·HCl] = 0, 0.72, and 4.0 M) were determined by DLS. These points were chosen since HPLC analysis (Figure 3) showed that only one species was present at these denaturant concentrations; this was also confirmed by our DLS measurements. The Stokes–Einstein equation for rigid spherical molecules was used to calculate R_S: $D = k_B T/6\pi\eta R_S$, where D is the translational diffusion coefficient, k_B is the Boltzmann constant, T is the absolute temperature, and η is the absolute viscosity of the solvent. The results are presented in Figure 4. Stokes radii determined by SEC–HPLC and DLS are in excellent agreement: native DnaK, 40 ± 2 and 41 ± 2 Å, respectively; DnaK in 0.72 M Gdn·HCl, 46 ± 2 and 47 ± 2 Å, respectively; and DnaK in 4.0 M Gdn·HCl, 68 ± 3 and 69 ± 4 Å, respectively.

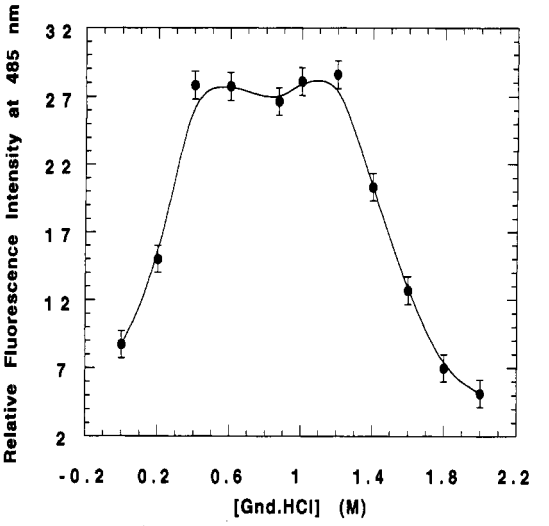

FIGURE 5: Binding of bis-ANS followed by fluorescence as a function of Gdn·HCl concentration. Mixtures of DnaK (1 μM), bis-ANS (1.4 μM), DTT (1 mM), and Gdn·HCl, prepared as indicated in the text, were equilibrated at 20.0 °C for 2 h, and the fluorescence spectra were determined; excitation was at 394 nm; excitation and emission slit widths were 4 and 10 nm, respectively.

Binding to Bis-ANS. We investigated the binding of bis-ANS to DnaK as a function of Gdn·HCl; the results are shown in Figure 5. In the absence of DnaK, bis-ANS has an emission maximum at 530 nm (excitation: 394 nm). A blue shift in the λ_{max} to 485 nm and an increase in intensity is observed in the presence of DnaK. In the Gdn·HCl concentration range 0.4–1.2 M, there is a marked increase in the fluorescence intensity at 485 nm, indicating preferential binding to the intermediate state.

DISCUSSION

Unfolding of DnaK Involves at Least One Intermediate State. The biphasic unfolding curves depicted in Figures 1B and 2B indicate that DnaK unfolding induced by Gdn·HCl does not proceed via a simple two-state mechanism, but rather it involves at least one stable intermediate state. Similar results have already been reported for the thermal denaturation of DnaK and bovine brain hsp73 (Palleros et al., 1991, 1992). In the absence of nucleotides, at Gdn·HCl concentrations between 0.6 and 1.0 M, DnaK still possesses most of its secondary structure as determined by far-UV CD (Figure 1); however, the environment around its only tryptophan residue (position 102) has been drastically altered in relation to that of the native state, since there is a substantial decrease in the fluorescence intensity at 335 nm and a red shift in the λ_{max} (Figure 2). No further change in tryptophan fluorescence is observed by increasing the Gdn·HCl concentration to 6.0 M, indicating that in 0.6 M Gdn·HCl this residue is already fully exposed to the solvent. The two-step transition observed by fluorescence intensity at 305 nm (Figure 2B) suggests that not all the tyrosines are perturbed by the solvent to the same extent, but rather some of them undergo a transition leading to solvent exposure at lower Gdn·HCl concentrations than the rest. That the denaturant-induced unfolding pathway of DnaK indeed proceeds via a stable intermediate state is made evident by the detection of three distinct species by SEC–HPLC whose relative amounts change as the denaturant concentration changes (Figure 3, peaks N, I, and U). In the

range 0.3–0.6 M Gdn·HCl species N and I coexist; the relative amount of N diminishes as the denaturant concentration increases. Between 0.6 and 1.0 M Gdn·HCl only species I is detected. Between 1.1 and 1.7 M Gdn·HCl two species (I and U) are detected. The fact that two different denatured states (I and U) are seen by SEC–HPLC indicates that their interconversion rate is slower than the time scale of the chromatographic separation; therefore a significant energy barrier must separate them.

The Intermediate State is Expandable. The decrease in the elution volume of I with increasing denaturant concentration (Figure 3) could, in principle, be ascribed to rapid association–dissociation of monomeric DnaK (in the I state) to form dimers, trimers, tetramers, etc. in a Gdn·HCl-dependent process. If these species are in rapid equilibrium they would be detected as a single peak by SEC–HPLC, whose elution volume decreases as the degree of association, and therefore the average particle size, increases. If this is the case, it would be expected that an increase in protein concentration, at fixed Gdn·HCl concentration, should also cause a decrease in the elution volume, since the association process is concentration dependent. No such shift in elution volume was observed over a range of concentrations covering a 50-fold increase in DnaK concentration (from 1.6 to 72 μM). Therefore oligomerization of the protein in the I state does not occur.

It has been observed that SEC elution volumes of native and unfolded forms of proteins decrease with increasing denaturant concentration (Shalongo et al., 1989; Withka et al., 1987; Shortle & Meeker, 1989; Corbett & Roche, 1984). This phenomenon has been attributed to different effects: changes in the permeation capabilities of the stationary phase (Shalongo et al., 1989; Shortle & Meeker, 1989); protein binding to the stationary phase (Shalongo et al., 1992), a point which we will discuss later; and true swelling of the protein due to binding of the denaturant (Withka et al., 1987; Corbett & Roche, 1984). We determined the void volume and the solvent-accessible volume of the HPLC column in the range of Gdn·HCl concentration used for the unfolding studies and found that there was no change in the void volume in the range 0–6 M Gdn·HCl and only a minor increase in the solvent-accessible volume as determined by the elution volume of sodium azide. These changes were taken into consideration when K_d was calculated.

It has been shown that SEC–HPLC elution volumes of native and denatured proteins may be affected by binding to the stationary phase (Shalongo et al., 1992). This process is minimized by increasing denaturant concentration, causing the protein to elute earlier from the column. However, on the basis of this model (Shalongo et al., 1992), the rate of K_d change for most proteins with increasing Gdn·HCl concentration is expected to be –0.01 per 1 M increase in the denaturant concentration (in the range [Gdn·HCl] = 0–5 M). Our results indicate that native, intermediate, and unfolded DnaK decrease their K_d values at rates of –0.05, –0.08, and –0.04 per 1 M increase in Gdn·HCl concentration, respectively. Therefore, the binding to the stationary phase cannot account for the large changes in partition coefficients observed for DnaK. It was shown (Corbett & Roche, 1984) for the same kind of stationary phase as used in our investigations that the correlation between the Stokes radius (measured independently) and the K_d values for more than 10 proteins under native and unfolding conditions (6 M Gdn·HCl or 8 M urea) falls on the same curve, indicating that SEC–HPLC gives a good estimation of hydrodynamic properties regardless of the solvent. That the decrease in K_d values reported here do indeed reflect changes in molecular size, was confirmed by DLS measurement of Stokes radii at three Gdn·HCl concentrations: 0, 0.72, and 4.0 M, where the native, intermediate and unfolded states, respectively, are favored. The agreement with SEC–HPLC values was excellent (Figure 4).

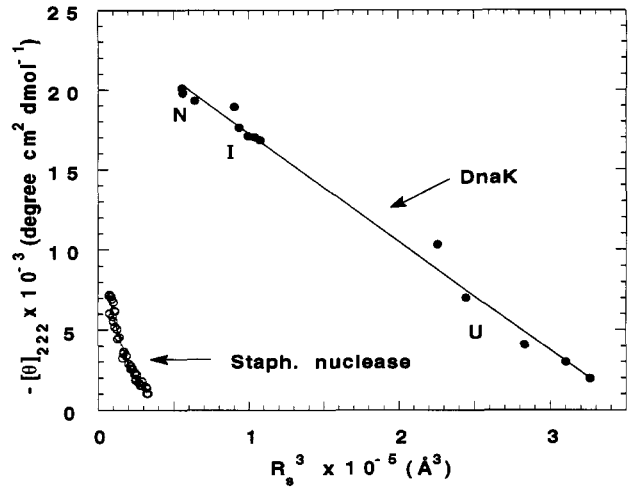

FIGURE 6: Correlation between the mean residue weight ellipticity at 222 nm and compactness. Ellipticity is plotted against R_S^3 for DnaK and fragment 1–128 of staphylococcal nuclease and its mutants V66L, G88V, V66L+G88V, and A69T+A90S. Mean residue weight ellipticities for staphylococcal nuclease fragments were calculated from Figure 6 of Shortle and Meeker (1989); R_S values of staphylococcal nuclease fragments were calculated using a linear correlation between elution volume and R_S of standard proteins from Figure 7 of Shortle and Meeker (1989).

The results presented in Figure 4 indicate that the Gdn·HCl-induced intermediate state of DnaK is highly expandable. At low Gdn·HCl concentration (ca. 0.4 M) its Stokes radius is only about 10% larger than that of the native state, which is consistent with the idea of a compact denatured state (molten globule); however, as the Gdn·HCl concentration increases, the Stokes radius also increases. At 1.34 M Gdn·HCl this intermediate is almost as large as the unfolded state, as can be seen by the closeness of the HPLC elution volumes. The Stokes radii calculated for the intermediate and the unfolded states in 1.34 M Gdn·HCl are 54 and 58 Å, respectively. This represents more than a 35% increase in radius of the intermediate compared to the native protein. The unfolded state also expands. The Stokes radius in 6 M Gdn·HCl is 69 Å, which represents a 20% increase compared to the unfolded state near the midpoint of the transition.

When the mean residue weight ellipticity at 222 nm is plotted against R_S^3, a linear relationship is obtained (Figure 6). This is a rather surprising result, since it implies that similar changes in ellipticity are accompanied by similar changes in molecular volume regardless of the state of the protein considered (N, I, or U). It also implies that the ellipticity at 222 nm may reflect the compactness of the polypeptide chain in addition to the content of secondary structure. In fact, the CD signal of an assembly of chromophores is sensitive to the relative orientation of the chromophores and the distance separating them. Although the modeling of actual proteins is, of necessity, a formidable task, some features of the CD dependence on molecular geometry can be revealed by simple models. For two identical interacting chromophores, it has been shown that the CD signal diminishes as the square of the distance between them (Tinoco & Cantor, 1970). Therefore, one can expect to see an increase in CD signal as the compactness of

the molecule increases, without invoking changes in the amount of secondary structure. In Figure 6 we also included data adapted from the literature for fragment 1–128 of staphylococcal nuclease and several of its mutants (Shortle & Meeker, 1989). Mutants V66L+G88V, V66L, and G88V are believed to unfold to a rather compact denatured state (Shortle & Meeker, 1989), whereas mutant A69T+A90S is believed to represent an ensemble of conformations with little residual structure that is lost gradually as the denaturant concentration increases (Shortle & Meeker, 1989). Despite these differences in structure, the plot of ellipticity at 222 nm vs R_S^3 gives a unique correlation for all these fragments. These results also support the idea that the ellipticity at 222 nm might reflect not only the amount of secondary structure but also the compactness of the molecule. Our data does not allow us to dissect the extent of each contribution to the ellipticity at 222 nm; we believe that such a dissection would be rather difficult, since it has been shown, from a theoretical standpoint, that compactness and amount of internal (secondary) structure are interrelated. Dill and co-workers (Dill & Shortle, 1991; Chan & Dill, 1989, 1990), on the basis of the theory for polymer chains, have predicted that helices, sheets, and turns should increase with the compactness of the molecule. The data in Figure 6 confirm such a prediction.

Unfolding Models. The results presented in this paper for the denaturant-induced unfolding of DnaK are open, in principle, to two different interpretations: (a) independent domain unfolding and (b) hierarchical unfolding.

Independent Domain Unfolding. In this model the biphasic transition observed by CD and the single transition seen by tryptophan fluorescence could be interpreted as the initial unfolding of the N-terminal domain (for which the tryptophan is a probe) with C_m = 0.5 M followed by the unfolding of the C-terminal domain (C_m = 1.6 M), which would be silent by tryptophan fluorescence. However, this hypothesis can be ruled out on the following grounds. (1) DnaK unfolding, followed by tyrosine fluorescence, also shows a two-step transition (C_m = 0.6 ± 0.1 and 1.5 ± 0.1 M), although all the tyrosines are confined to the N-terminal domain. (2) If we consider the ellipticity at 222 nm as an indication of solely secondary structure content, the first transition observed by far-UV CD accounts for only a 15% loss of secondary structure. Although the 3-D structure of DnaK is not known, estimation of α-helix and β-sheet content by the method of Garnier et al. (1978) shows that 62% of the total content of α-helix and β-sheet in DnaK is present in the N-terminal domain, and 38% is in the C-terminal domain (when this method is applied to the N-terminal domain of bovine brain hsp73, it gives results that agree reasonably well with the 3-D structure already reported; Flaherty et al., 1990, 1991). Therefore, a decrease of only 15% in signal at 222 nm, as observed in the first transition, is hardly compatible with the unfolding of the N-terminal domain, which should account for more than 60% of the secondary structure of DnaK. (3) The N-terminal domain is known to be more resistant to proteases than the C-terminal domain (Chappell et al., 1987) and therefore should be more stable than the C-terminal domain.

Within the independent domain unfolding hypothesis, another model is possible, i.e., that the C-terminal domain unfolds first. This would be consistent with points 2 and 3 above, but it would require the tryptophan residue and some of the tyrosines to be buried at the interface of the N-terminal and C-terminal domains. The unfolding of the C-terminal domain will then expose the aromatic residues to the solvent, causing a decrease in their fluorescence intensity. Our results indicate that upon ATP or ADP binding there is a shift in the first transition to higher C_m. There is little effect on the C_m of the second transition. This model would then require that the binding of nucleotides, which is known to occur in the N-terminal domain, translate exclusively into an increase in the stability of the C-terminal domain, with little or no effect on the stability of the N-terminal domain. This scenario seems very unrealistic. Finally, the independent domain unfolding model can account neither for the continuous increase in the Stokes radius as the Gdn·HCl concentration increases nor for the binding of bis-ANS. Bis-ANS, a dimer of ANS, is known to bind to hydrophobic regions of proteins and is very sensitive to small conformational changes of the protein (Musci & Berliner, 1985; Musci et al., 1985). This kind of fluorescent probe binds tightly to molten globule states (Goto & Fink, 1989). The results presented in Figure 5 indicate that this fluorescence probe does not bind significantly to the native and the unfolded states of DnaK; binding is maximal in the Gdn·HCl range 0.4–1.2 M, where the intermediate state is favored. If this intermediate state were composed of an unfolded domain plus a folded domain, binding would not be expected.

Hierarchical Unfolding. In this model, the native conformation is assumed to be formed by a number of structural units or building blocks. Each building block consists of regions of secondary structure stabilized through side-chain interactions. These building blocks may be domains, subdomains, or autonomous folding units (Shoemaker et al., 1987) connected by loops and segments of unordered structure and tightly packed together via tertiary interactions. For proteins with several structural units, the denaturant would first *break* contacts between units (interunit interactions) and would only *weaken* side-chain interactions within the unit (intraunit interactions). This would result in an intermediate state with a low content of tertiary structure, since most of the side-chain contacts between units are lost, but with a relatively high content of secondary structure stabilized by intraunit interactions (e.g., the rolling interactions between the hydrophobic sides of two amphiphilic helices; Baldwin, 1991). This intermediate would also be expandable without losing its stability as more solvent molecules penetrate the *interunit space*. Finally, as the solvent starts to disrupt the stabilizing interactions within the structural unit, the protein would unfold. This model makes implicit the existence of two kinds of tertiary (and perhaps secondary) structure: interunit and intraunit. The interunit structure would be the first to be disrupted by the solvent; on the other hand, the intraunit structure, more protected from interactions with the medium, would be more resistant to higher denaturant concentrations. For small proteins with only a few or perhaps one structural unit, *compact* intermediates would be the only species detected, since the molecule could not expand significantly without losing its stabilizing intraunit interactions. This model can accommodate the formation of intermediate states such as molten globules.

Within this hypothesis, DnaK would first lose most of its tertiary structure (first transition) due to the disruption of side-chain interactions between structural units. Then, as the denaturant concentration is increased, most of its secondary structure and the remaining tertiary structure within each building block would be lost (second transition). The observed change in ellipticity at 222 nm associated with the first transition (15% of signal) could be explained as the contribution of the aromatic side chains to this portion of the CD

spectrum (Sears & Beychok, 1973), although a change in secondary structure cannot be ruled out.

For a number of proteins, intermediate states obtained at low pH and moderate ionic strength (Goto & Fink, 1989; Gast et al., 1986) have been shown to be compact and to fit the definition of "molten globules". However, for multidomain proteins, the hypothesis of a *compact* denatured state *in equilibrium* with the native (or unfolded) state has not previously been substantiated when denaturants such as Gdn·HCl or urea are involved. Ptitsyn and co-workers (1990) have shown that a *kinetic* intermediate of staphylococcal β-lactamase is compact, according to its SEC elution volume. However, this intermediate was obtained under far-from-equilibrium refolding conditions at low Gdn·HCl concentrations. At higher denaturant concentrations, where the *equilibrium* intermediate was stable, the reported SEC elution volume was significantly smaller than that for the kinetic intermediate (Ptitsyn, 1990), in agreement with our findings of molecular volume expansion as a function of denaturant concentration. Our HPLC results for DnaK also indicate that the kinetic intermediate is more compact (R_S= 43 ± 2 Å) than the thermodynamic intermediate obtained in the Gdn·HCl concentration range 0.4–1.4 M.

The data presented here indicate that the intermediate state, I, of DnaK possesses some of the characteristics of a "molten globule", i.e., similar content of secondary structure to the native state and weakened tertiary structure. However, the HPLC data, as discussed above, do not support the idea of a *unique* compact intermediate state. The results indicate a continuous increase in the molecular volume of the intermediate state as well as the unfolded state with increasing denaturant concentrations. These results suggest that both the intermediate and unfolded states are two *ensembles* of conformations, separated by an energy barrier, whose average dimensions shift with Gdn·HCl concentration. At low Gdn·HCl concentrations, near the midpoint of the first transition, the intermediate state is indeed compact and fits the definition of a molten globule. However, as the denaturant concentration is increased, it expands to almost the same size as the unfolded protein; near the midpoint of the second transition, the intermediate and unfolded states are very close in hydrodynamic size. The existence of such swollen species was predicted by Finkelstein and Shakhnovich (1989). On the basis of the thermodynamics of protein–solvent interactions these authors showed that solvent penetration causes the molten globule to expand gradually without any phase transition. The swollen intermediate then undergoes a second-order phase transition to the coil (unfolded) conformation; this model does not account for variations in ordered structure. The results discussed here indicate that molten globules are a special case of a larger family of intermediates that possess a high content of secondary structure and some residual or fluctuating tertiary structure.

ACKNOWLEDGMENT

We are grateful to Dr. R. Pecora and Mr. E. Hanson from Stanford University for their invaluable help with the DLS experiments. We thank Dr. Linda DeYoung for helpful discussions during the course of these studies.

REFERENCES

Baldwin, R. L. (1991) *Chemtracts: Biochem. Mol. Biol. 2*, 379–389.

Bardwell, J. C. A, & Craig, E. A. (1984) *Proc. Natl. Acad. Sci. U.S.A. 81*, 848–852.

Cegielska, A., & Georgopoulos, C. (1989) *J. Biol. Chem. 264*, 21122–21130.

Chan, H. S., & Dill, K. A. (1989) *Macromolecules 22*, 4559.

Chan, H. S., & Dill, K. A. (1990) *Proc. Natl Acad. Sci. U.S.A. 87*, 6388.

Chappell, T. G., Konforti, B. B., Schmid, S. L., & Rothman, J. E. (1987) *J. Biol. Chem. 262*, 746–751.

Christensen, H., & Pain, R. H. (1991) *Eur. Biophys. J. 19*, 221–229.

Cleland, J. L., & Wang, D. I. C. (1990) *Biochemistry 29*, 11072–11078.

Corbett, R. J. T., & Roche, R. S. (1984) *Biochemistry 23*, 1888–1894.

Creighton, T. H., & Pain, H. R. (1980) *J. Mol. Biol. 137*, 431–436.

Dill, K. A., & Shortle, D. (1991) *Annu. Rev. Biochem. 60*, 795–825.

Finkelstein, A. V., & Shakhnovich, E. I. (1989) *Biopolymers 28*, 1681–1694.

Flaherty, K. M., DeLuca-Flaherty, C., & McKay, D. B. (1990) *Nature 346*, 623–628.

Flaherty, K. M., McKay, D. B., Kabsch, W., & Holmes, K. C. (1991) *Proc. Natl. Acad. Sci. U.S.A. 88*, 5041–5045.

Gaitanaris, G. A., Papavassilou, A. G., Rubock, P., Silverstein, S. J., & Gottesman, M. E. (1990) *Cell 61*, 1013–1020.

Garnier, J., Osguthorpe, D. J., & Robson, B. (1978) *J. Mol. Biol. 120*, 97–120.

Gast, K., Zierwer, D., Welfe, H., Bychkova, V. E., & Ptitsyn, O. B. (1986) *Int. J. Macromol. 8*, 231–236.

Goto, Y., & Fink, A. L. (1989) *Biochemistry 28*, 945–952.

Kuwajima, K. (1989) *Proteins 6*, 87–103.

Kuwajima, K., Nitta, K., Yoneyama, M., & Sugai, S. (1976) *J. Mol. Biol. 106*, 359–373.

Langer, T., Lu, C., Echols, H., Flanagan, J., Hayer, M. K., & Hartl, F. U. (1992) *Nature 356*, 683–689.

Landry, S. J., Jordan, R., McMacken, R., & Gierasch, L. M. (1992) *Nature 355*, 455–457.

Lehrman, S. R., Tuls, J. L., Havel, H. A., Haskell, R. J., Putnam, S. D., & Tomich, C. S. C. (1991) *Biochemistry 30*, 5777–5784.

Liberek, K., Skowyra, D., Zylicz, M., Johnson, C., & Georgopoulos, C. (1991) *J. Biol. Chem. 266*, 14491–14496.

Matthews, C. R., & Crisanti, M. C. (1981) *Biochemistry 20*, 784–792.

McCarty, J. S., & Walker, G. C. (1991) *Proc. Natl. Acad. Sci. U.S.A. 88*, 9513–9517.

Mitchinson C., & Pain, R. H. (1985) *J. Mol. Biol. 184*, 331–342.

Mitraki, A., Betton, J. M., Desmadoil, M., & Yon, J. M. (1987) *Eur. J. Biochem. 163*, 29–34.

Musci, G., & Berliner, L. J. (1985) *Biochemistry 24*, 3852–3856.

Musci, G., Metz, G. D., Tsunematsu, H., & Berliner, L. J. (1985) *Biochemistry 24*, 2034–2040.

Nozais, M., Bechet, J. J., & Houadjeto, M. (1992) *Biochemistry 31*, 1210–1215.

Nozaka, M., Kuwajima, K., Nitta, K., & Sugai, S. (1978) *Biochemistry 17*, 3753–3758.

Nozaki, Y. (1972) in *Methods in Enzymology* (Hirs, C. H. W., & Timasheff, S. N., Eds.) Vol. 26, p 43, Academic Press, New York.

Palleros, D. R., Welch, W. J., & Fink, A. L. (1991) *Proc. Natl. Acad. Sci. U.S.A. 88*, 5719–5723.

Palleros, D. R., Reid, K. L., McCarty, J. S., Walker, G. C., & Fink, A. L. (1992) *J. Biol. Chem. 267*, 5279–5285.

Ptitsyn, O. B. (1987) *J. Protein Chem. 6*, 273–293.

Ptitsyn, O. B. (1992) in *Protein Folding* (Creighton, T. E., Ed.) pp 243–300, W. H. Freeman & Company, New York.

Ptitsyn, O. B., Pain, R. H., Semisotnov, G. V., Zerovnik, E., & Razgulyaev, O. I. (1990) *FEBS Lett. 262*, 20–24.

Robson, B., & Pain, R. H. (1976) *Biochem. J. 155*, 331–344.

Saito, Y., & Wada, A. (1983) *Biopolymers 22*, 2123–2132.

Sears, D. W., & Beychok, S. (1973) in *Physical Principles and Techniques of Protein Chemistry*, Leach, S., Ed.) Part C, Chapter 23, Academic Press, New York.
Shalongo, W., Jagannadham, M. V., Flynn, C., & Stellwagen, E. (1989) *Biochemistry 28*, 4820–4825.
Shalongo, W., Heid, P., & Stellwagen, E. (1993) *Biopolymers 33*, 127–134.
Sherman, M. Y., & Goldberg, A. L. (1991) *J. Bacteriol. 173*, 7249–7256.
Shoemaker, K. R., Fairman, R., Kim, P. S., York, E. J., Stewart, J. M., & Baldwin, R. L. (1987) *Cold Spring Harbor Symp. Quant. Biol. 52*, 391–398.
Shortle, D., & Meeker, A. K. (1989) *Biochemistry 28*, 936–944.
Skowyra, D., Georgopoulos, C., & Zylicz, M., (1990) *Cell 62*, 939–944.
Tanford, C. (1968) *Adv. Protein Chem. 23*, 121–282.
Tinoco, I., Jr., & Cantor, C. R., (1970) *Methods Biochem. Anal. 18*, 81.
Withka, J., Moncuse, P., Baziotis, A., & Maskiewicz, R. (1987) *J. Chromatofr. 398*, 175–202.
Yutani, K., & Ogasahara, K. (1980) *J. Mol. Biol. 144*, 455–465.
Zerovnik, E., Jerala, R., Kroon-Zitko, L., Pain, R. H., & Turk, V. (1992) *J. Biol. Chem. 267*, 9041–9046.